Research Article   **Open Access**

Catheter Based Renal Sympathetic Denervation by Segmental Endoluminal Laser Radiation in a Pig Model: Anatomical and Histopathological Results

Sagerer-Gerhardt M[1,2], Haider W[3], Matiasek K[4] and Weber HP[*1]

[1]CCEP - Center Taufkirchen, Section Research, Development, Education, Schlesierstrasse 4, Taufkirchen, DE-82024, Germany

[2]Departments of Anesthesiology, Hospital Neuperlach, Teaching Hospital of the LM, University of Munich, Oscar-Maria-Graf-Ring 51, Munich, DE-81737, Germany

[3]Institute for Veterinary Pathology, Schoenhauser Strasse 62, Berlin, DE-13127, Germany

[4]Section Head of Clinical & Comparative Neuropathology, Centre of Clinical Veterinary Medicine, Ludwig Maximilians University Munich, Veterinarstrasse 13, Munich, DE-80539, Germany

[*]**Corresponding author:** Weber HP, Director, CCEP Centre Cardiovascular Laser Application Taufkirchen, Schlesierstrasse 4, DE-82024 Germany, Fax: +49 (0)89 759 5770, Tel: +49 (0)89 759 5596, E-mail: hw@ccep.de

Abstract

For renal sympathetic laser denervation (RSLD) we have tested endoluminal, segmental, laser catheter radiation of renal arteries by using continuous wave 1064nm Nd:YAG laser light. A total of 74 laser impacts at 15 to 20W/15-80 s (4.5 to 30 J/mm²) were applied in the left (n=34) and the right (n=40) renal artery in 6 anesthetized healthy pigs by using the open irrigated laser catheter *RytmoLas®* (CE 0481), introduced via the femoral artery and manipulated under X-ray control towards the renal arteries by means of a steerable AGILIS sheath. The laser beam illuminated homogenously an arterial segment at a length of up 6.0 mm. Level of energy applied was adapted to endovascular surfaces measured and calculated after renal angiography. After a 3-4 hours observation time in 4 pigs, and after 28 days, and 31 days of follow-up in two pigs, control angiograms were performed and renal arteries were removed, examined gross pathologically, histopathologically, and electron microscopically. Thermal damages were conspicuous in all of the nerves in the irradiated vessel segments regardless of the level of energy applied and of their distances from the endoluminal artery surface. However, also mild thermal damages of the vessel wall were conspicuous acutely in some of the arteries. After long-term follow-up permanent RSLD was conspicuous histopathologically and electron microscopically whereas arterial damages were found normal or being in a final healing process. For evaluation of this healing process a longer follow-up is needed. RSLD can achieve selective and permanent renal denervation without long-term collateral damages. Provided these results can be confirmed by clinical trials RSLD may become an intriguing alternative for renal denervation in patients with resistant hypertension.

Keywords: Renal Sympathetic Laser Denervation; Laser; Resistant Hypertension; Renal Denervation

Introduction

Hypertension (HT) is an epidemic affecting 1.39 billion people. It is the commonest risk factor for premature death and disability worldwide [1]. HT is also an important health challenge because of its prevalence and resulting cardiovascular and chronic kidney diseases [2,3]. Since 2000 HT is increasing in low and middle-income countries, but it is steady or decreasing in high income countries [4-7]. However, up to one-in-five treated patients are deemed to be treatment resistant on at least three different antihypertensive medication classes, including diuretics, or have serious side effects, or refuse drug treatment [8-12]. Renal sympathetic nerve hyperactivity is a key to pathogenesis of essential HT. Activation of the sympathetic nervous system (SNS) is recognized to occur in all stages of HT and correlates to its severity [13,14]. Renal denervation (RD), a minimally invasive catheter based procedure, has been suggested as an effective, evidence-based approach for controlling resistant HT [15]. Catheter ablation of renal nerves has shown efficacy in reducing blood pressure without procedural mortality [16,17]. In a review, current technologies of RD were described, including Radiofrequency current, Ultrasound, Cryoballoon, and Ionizing Radiation neural ablation [18], periarterial ethanol injection [19], and, by using Laser light as well [20]. In our study we have investigated a novel catheter based Renal Sympathetic Laser Denervation technique (RSLD) in a pig model.

Materials and Methods

For transcatheter intraluminal segmental renal artery laser radiation a continuous wave 1064 nm *mediLas fibertom 4060 N* laser Dornier MedTech, Wessling, Germany was used. Laser light was applied via an 8F open-irrigated Laser catheter *RytmoLas®* LasCor GmbH Taufkirchen, Germany (CE 0481), described in detail elsewhere [21]. The laser catheter was manipulated by means of a steerable AGILIS™ NxT Small, 16.8 mm, 40cm sheath, St. Jude Medical, USA. Experiments were performed in the Center for Preclinical Research (ZPF) of the Technical University of Munich; Director Prof. Dr. Christine Baumgartner.

Animal preparation

Six healthy pigs, 3 female and 3 male, weighing 30 to 56 kg (average 39 kg) were including in the study. The investigations comply with the principles outlined in the Declaration of Helsinki. Animal experimental studies were conforming to the Directive 86/609/EEC on the protection of animals used for experimental and other scientific purposes, adopted in 1986 by the European Commission; and were approved by the Ethics committee of the TUM University of Munich. One day bevor the experiment each of the animals received 250 mg Aspirin orally. Prior to the experiment 10-15 mg/kg Ketamin + 2 mg/kg Azaperon + 1 mg Atropin i.m. injection was done in the transport box. Under sedation the animals were fixed in supine position on the operating table and after venous access through a small ear vein anesthesia was started with i.v. Propofol 1%, 1.5mg/kg, and, in addition, i.v. Metamizol 40 mg/kg for analgesia. After intubation the animals were ventilated with a mixture of room-air and oxygen and anesthesia was maintained by Propofol 2%. Respiratory and circulatory parameters were continuously monitored including gas-check with end-respiratory CO_2 control, Pulseoximetry, Kapnometry, rectal temperature, electrocardiograms and invasive blood pressure monitoring. Fluid restitution by infusion with electrolyte 10 ml/kg/h and intraoperatively for anticoagulation i.v. Heparin 150 IU/kg and Aspirin 250 mg were given. Analgesia during the procedure was maintained with Fentanyl 0.015mg/kg and after the anesthesia with Buprenorphin 0.2mg/kg. Shortly after recovery from the anesthesia the animals received also i.v. Carprofen 4mg/kg. All the animals were normotensive and in normal sinus rhythm prior to the experiments.

The skin in the left or right groin was incised; the femoral artery exposed and supported in a sling. The artery was incised and a guidewire was inserted and advanced under X-ray control up to the abdominal aorta. The steerable AGILIS sheath was flushed with saline and was introduced with dilator over the guide wire into the femoral artery and was advanced under X-ray control into the abdominal aorta. Guide wire and dilator were removed and after abdominal angiography a renal artery was catheterized under X-ray guidance so that the tip of the sheath was positioned in the root of the renal artery. Selective renal artery angiogram was performed and diameter and length of the main renal artery were measured on the screen (Figure 1). Measurements were used for calculation of endovascular surfaces and for calculation of the energy density adapted to the endoluminal surface (Figure 2). Power levels at 15 and 20 Watts were applied. In order to achieve the same energy density with the same power, radiation times in larger arteries were longer. A table with energy densities calculated for various arterial diameters prior to the study allowed for a quick decision on adequate radiation times during the experiments. For evaluation of the laser effects on nerves and on the vessel wall incremental energy densities from 4.5 J/mm² up to 30 J/mm² were applied.
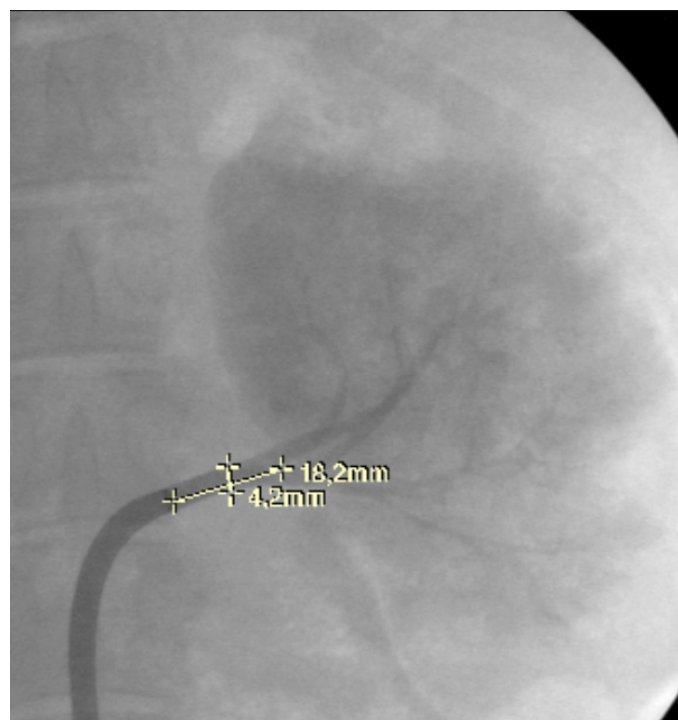

Figure 1: Left renal angiogram of a pig showing artery measurements: length = 18.2mm, diameter = 4.2 mm, used for calculation of energy density (see Figure 2)
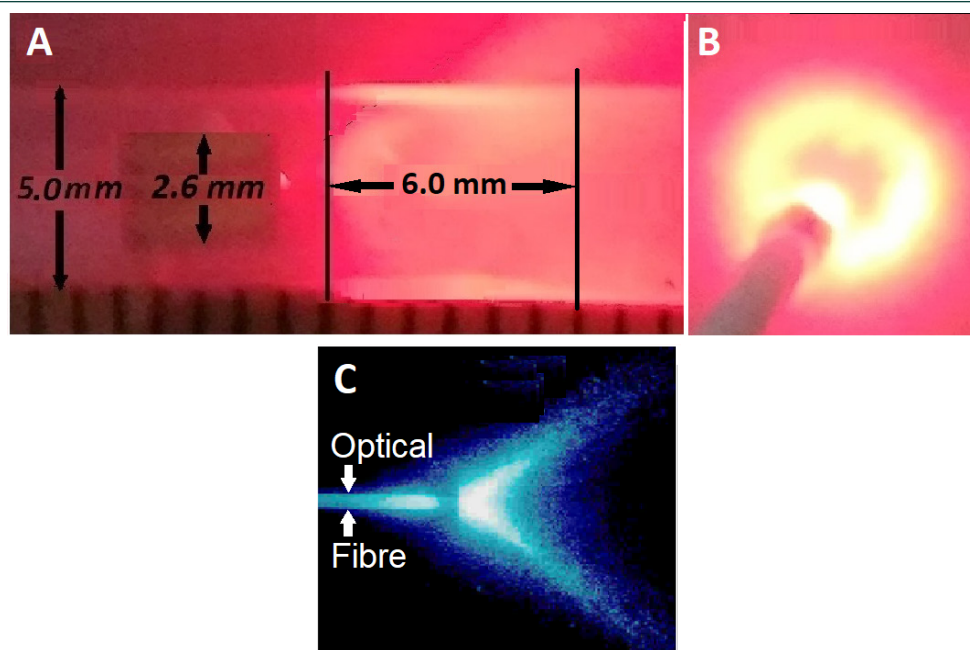
Figure 2: Example for the calculation of energy density **(A)** The 8F catheter RytmoLas® fed into a plastic tube is emanating a HeNe pilot beam illuminating the inner lumen of the tube at a length of 5-6mm = 78-95mm². Radiation at 15W = 0.20-0.16 W/mm² with a radiation time of 50s will achieve approximately 8-10 J/mm²; **(B)** Frontal view of the pilot beam showing a "Donut" –like circular spot illuminating a tube segment upto 6mm; **(C)** The genuine 1064nm Nd:YAG laser beam

The Laser catheter was connected to the rolling pump of the laser and was flushed continuously with saline 15 ml/min. Then, it was inserted through the hemostatic valve of the AGILIS sheath and advanced under X-ray control with its tip 2.0 to 3.0 mm beyond the endhole of the sheath. Kept in stable position within the sheath, sheath and catheter were advanced into the lumen of the main renal artery up to its main ramification. With the start of laser application catheter irrigation was automatically increased via the laser foot switch from 15 ml to 35 ml/min and returned to the continuous flow of 15 ml/min automatically with the release of the foot switch; the stop of the laser radiation.

No. sex	Left renal artery		Right renal artery	
Postoperative observation time 3-4 hours				
1 f	**4.5 J/mm²**	**10 x 15 W/Seconds**	**6.0 J/mm²**	**8 x 20 W/Seconds**
		2 x 25		1 x 17
		2 x 30		2 x 25
56 kg		1 x 15		2 x 30
		3 x 20		3 x 40
		2 x 40		
2 f	**10 J/mm²**	**4 x 20 W/Seconds**	**20 J/mm²**	**8 x 20 W/Seconds**
		2 x 24		2 x 40
43 kg		1 x 27		3 x 48
		1 x 28		1 x 55
				2 x 80
3 f	**10 J/mm²**	**7 x 15 W/Seconds**	**10 J/mm²**	**7 x 20 W/Seconds**
40 kg		4 x 25		6 x 30
		3 x 15		1 x 44
4 m	**10 J/mm²**	**4 x 15 W/Seconds**	**15 J/mm²**	**6 x 15 W/Seconds**
35 kg		4 x 50		6 x 75
Postoperative follow-up 28 (No 5) and 31 days				
5 f	**30 J/mm²**	**5 x 15 W/Seconds**	**15 J/mm²**	**6 x 15 W/Seconds**
31 kg		5 x 80 *pause 5-10 s* 80		6 x 80
6 m	**30 J/mm²**	**4 x 15 W/Seconds**	**15 J/mm²**	**4 x 15 W/Seconds**
30 kg		4 x 72 *pause 5-10 s* 72		4 x 72

Table 1: A total of 74 continuous wave Nd:YAG 1064nm endoluminal laser applications were aimed at the renal arteries of 6 pigs, left = 35, right = 39, with increasing levels of energy densities from 4.5 J to 30 J/mm² by using the open-irrigated ELMA laser catheter *RytmoLas®*

Laser applications were repeated at intervals of 5-10 seconds during a 4 to 5 mm stepwise withdrawal of the sheath and catheter from the ramification towards the artery root. The laser catheter was always kept in stable position inside the sheath. However, the laser catheter itself was pushed beyond the endhole of the sheath from the main ramification and was advanced into a major branch of the renal artery. Here laser applications were started with the catheter tip in wedge position close to the kidney hilum and consecutive laser impacts were applied by withdrawing the catheter into the sheath maintained in its position at the level of the artery ramification. Depending on the length of the main renal artery 4 to 10 overlapping laser impacts with various energy densities were applied (Table 1).

Subsequently, the laser catheter was removed and the procedure was repeated on the contralateral side. Eventually, the laser catheter was removed from the sheath, inspected for possible damages and checked for its function. The sheath was withdrawn in the aorta and after 4-5 hours, while still under anesthesia, a second selective renal artery angiogram was performed.

Subsequently, four animals received i.v. 0.1 ml/kg Pentobarbital and 40 ml KCl, the abdomen was opened, the kidneys with artery and the abdominal aortic segment were exposed and photo documented in situ. Kidneys and renal arteries with the adjacent connective and fatty tissue and the aortic segment were removed and were prepared for gross pathological and histopathological examination. The specimen were fixed in 10% neutral buffered formalin to be examined after hematoxylin and eosin (HE)-staining. For histopathological and electron microscopically examination a total of 104 arterial cross sections were performed at distances of 0.5 mm from each other in the irradiated vessel segments. Specimens were also prepared for scanning electron microscopy by a primary fixation with aldehydes before further processing with osmium tetroxide fixation, followed by dehydration with ethanol and drying.

Two of the six animals were prepared for a 4 weeks follow-up by antibiotic prophylactic medication with subcutaneous injection of 10mg/kg Enrofloxacin prior to be allowed to recover from the anesthesia. Venous lines were removed and the vessels ligated. During the 4 weeks follow-up period the two animals received antiplatelet medication 250mg/day Aspirin. After the follow-up period the animals were again anesthetized for hemodynamic, electrocardiographic, for laboratory check-up, and for renal angiograms, followed by Euthanasia and by harvesting of specimens as described above. For statistics mean and standard deviation were calculated.

Results

ECG-monitoring

ECG-monitoring showed normal tracings throughout the experiments except a few monomorphic ventricular extrasys-toles and couplets in 4 pigs. During the procedures increased heart rate of mean 114 ± 19 decreased to 86 ± 17 bpm after 50-60 minutes (p = 0.52), except in two animals: in one heart rate increased with 32% and degenerated in a tach-yarrhythmia that was successfully ended with 50 mg i.v. Amiodaron, and in a second animal that developed Hyperther-mia with a body temperature up to 42 °C and heart rate increased with 46%. The pigs were normotensive prior to the experiments. During the experiments systolic and diastolic blood pressure was 156 (±16) / 100 (±14) and decreased to 116 (±6.6) / 70 (±19) mmHg after the 3-4 hours observation time.

Angiographically

Angiographically Except in one pig with aberrant left artery renal arteries was normal. Diameters of irradiated renal artery segments ranged from 4.2 to 5.5 mm (4.9 ± 0.34) before laser application and were unchanged thereafter. There was no evidence of spasm, narrowing of the lumen or aneurysm formation following laser application including the angiograms of the pigs after the 4 weeks follow-up (Figure 3).
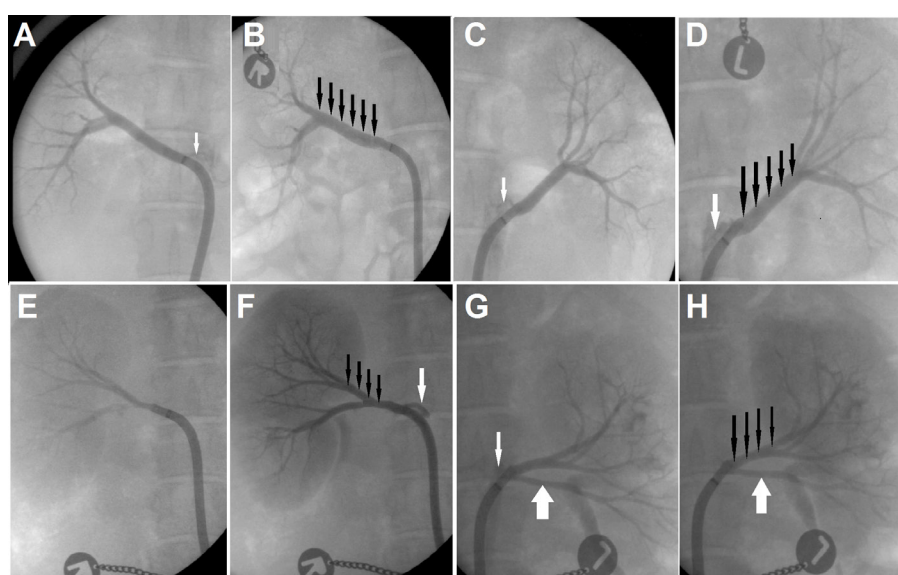

Figure 3: Renal artery angiograms prior to (A,C,E,G) and 4 weeks after (B,D,F,H) laser applications, once at 15 J/mm² (**B** 6X15W/80S, **F** 4X15W/72s), twice 2 X 30 J/mm² (**D** 5X15W/80s, **H** 4X15W/72S, at intervals of 5 seconds), ***showing***: unchanged normal aerial lumens after, as compared to those prior to laser applications (black vertical arrows). Aberrant left renal artery branch (thick white arrow in G, H), and dye reflux into the aorta (thin white vertical arrows)

Gross pathology

Gross pathology of the exposed specimen showed normal anatomy of the renal arteries from their aortic root up to the renal hilum. However, after laser applications with the catheter tip in wedge position in a renal artery branch renal lesions of coagulation necrosis were conspicuous whereas the vessel itself was undamaged (Figure 4).
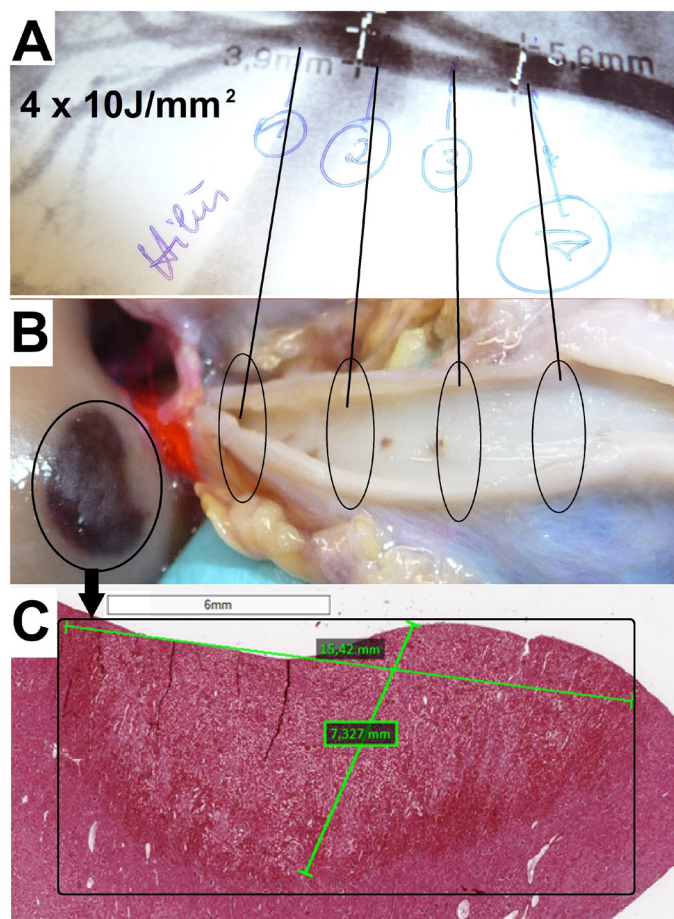

Figure 4: (A) Angiogram of the inferior branch of the right renal artery after 4 laser applications at 10 J/mm² each; (B) the opened artery after laser application ***showing*** a normal vessel wall. Positions of the catheter endhole during laser applications are marked by ovals. A dark spot of renal coagulation produced through the arterial wall is conspicuous (oval); (C) Hispathology of the clear cut acute laser lesion induced

Histopathology and Electron microscopy

Histopathology and Electron microscopy regardless of the level of energy density applied; in all of the nerves located around the irradiated vessel segments laser induced thermal damages such as edema, vacuolation, coagulation and total destruction/coagulation of nerves were conspicuous. Most severe damages were produced in nerves located 3-5 mm from the inner lumen of the irradiated vessel. After 4 weeks of follow-up histopathology demonstrated irreversibility of the laser induced lesions (Figure 5); findings that were confirmed electron-microscopically in the acute (Figure 6) and in the chronic specimen as well (Figure 7).

In general desquamations of the vessel intima was present. In addition, in three histological sections rupture of intima and media and slight intramural bleeding was conspicuous. The renal artery in some instances disclosed cracks of the intima and media, and, in three instances also intramural bleeding. All the above mentioned most probably caused by catheter manipulation. However, also slight to moderate laser induced thermal damages of the vessel wall were seen, especially when energy settings with powers at 20W were used. Importantly, healing process of traumatic and thermal vessel injuries is almost completed after 4 weeks of follow-up (Figure 8); anatomic integrity of the renal artery always was preserved including specimens radiated with highest energy densities (Figure 9).
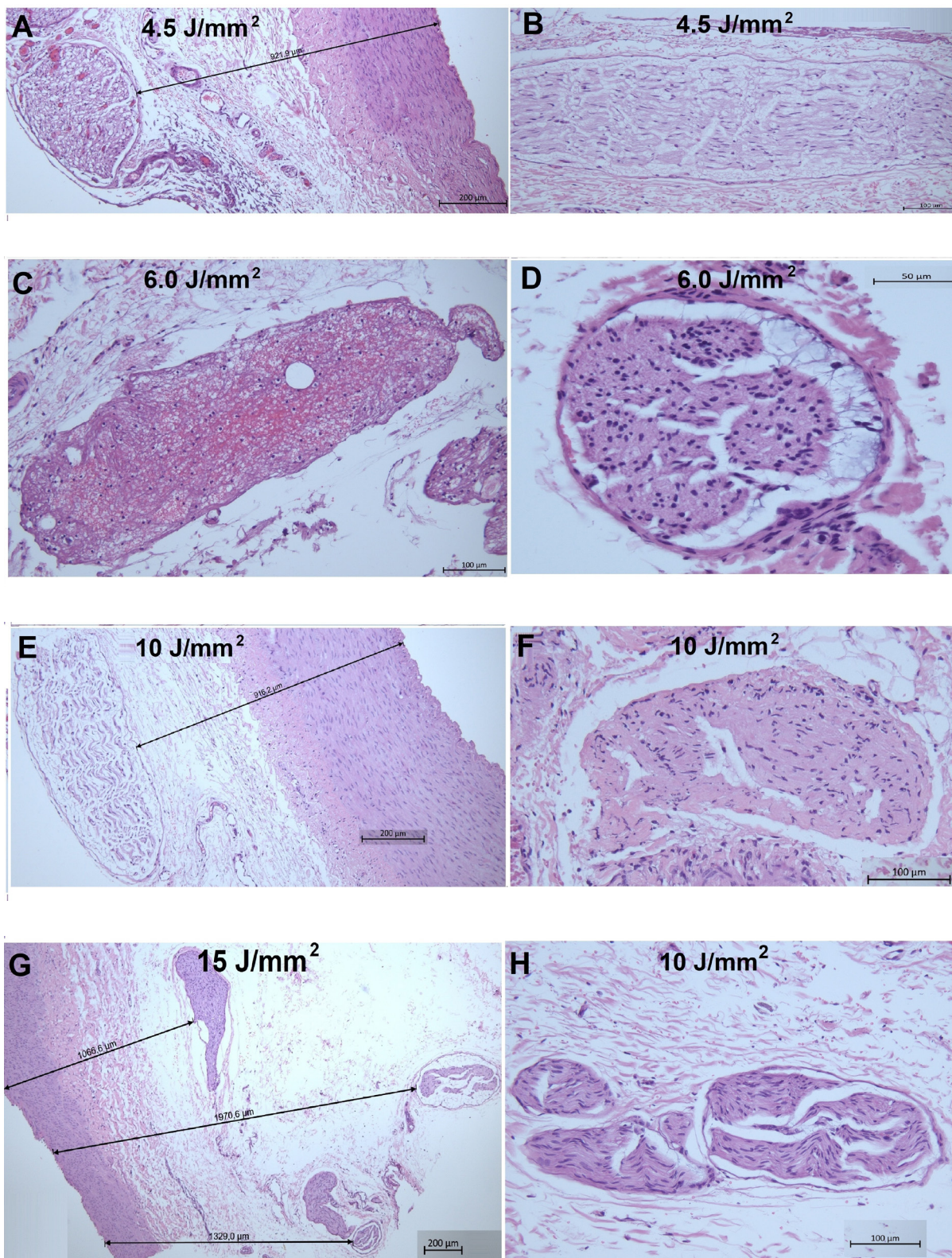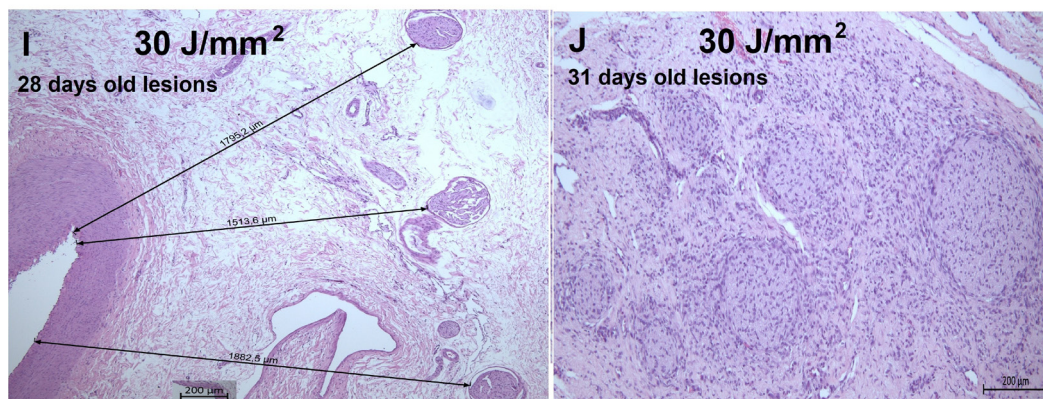
Chronic lesions

Figure 5: 4 hours old laser lesions of renal sympathetic nerves **(A)** Nerve with severe thermal alteration, vacuolation and hyperemia. Mild to moderate thermal damages of perirenal connective tissue, minimal bleeding into the fatty tissue, but normal layers of the renal arterial wall itself; **(B)** Longitude section through a nerve with severe edema, schistasis and disintegration of nerve fibres; **(C)** Completely thermally destroyed nerve; **(D)** Severe thermal alteration, edema and pyknotic nuclei; **(E)** Severe thermally damaged nerve, normal layers of renal artery wall; **(F)** Nerve with thermally induced schistasis, vacuolation, and pyknotic nuclei; **(G)** With an increasing distance from the arterial wall nerves show an increasing severity of thermal damages; **(H)** Nerves with thermally induced schistasis and edema; **(I)** Thermally injured nerves with schistasis at various distances from a normal renal artery; **(J)** Group of severely injured sympathetic nerves without coats, surrounded by proliferation of fiber generating cells
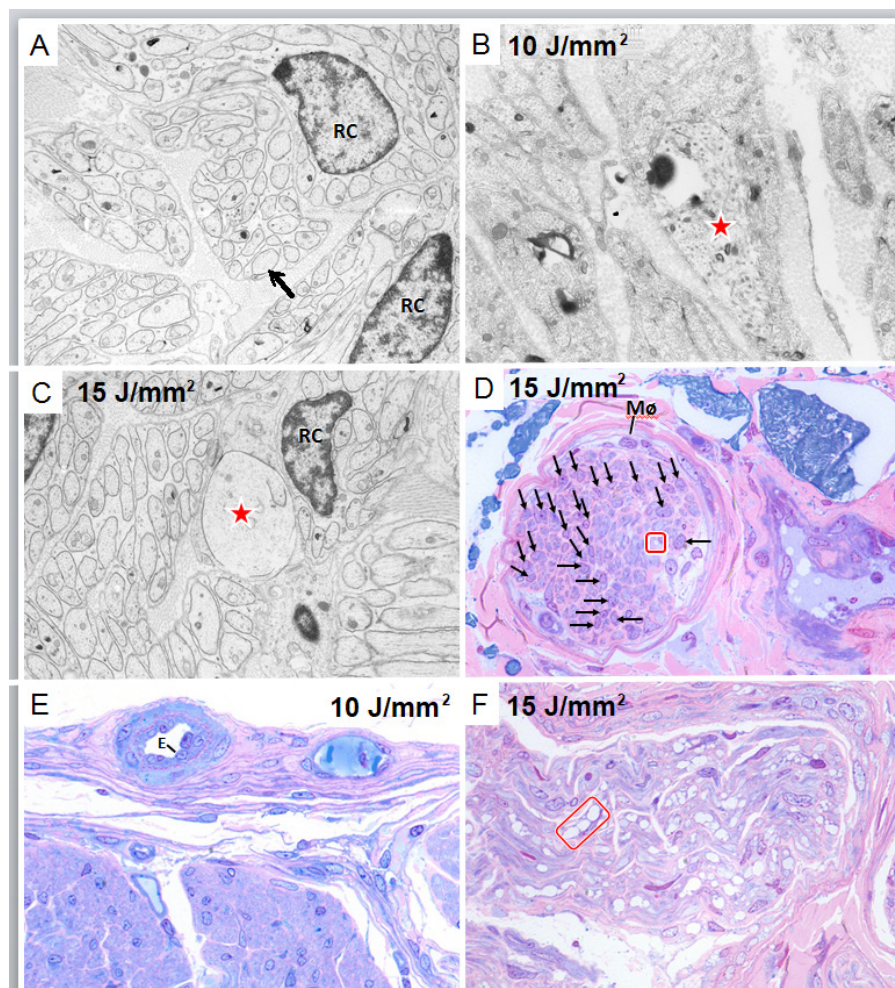

Figure 6: (A) Electron microscopically normal appearance of Remak cells (RC) and unmyelinated axons (arrow) around a nonradiated renal artery; **(B)** in contrast, after laser granular disintegration of unmyelinated axon containing electron denseinclusions (asterix); **(C)** Granular disintegration of otherwise regular unmyelinated axon (asterix); **(D)** Early, and **(E)** Advanced remak cell denervation with vacuolation (multiple arrows), and remake cell hyperplesia (right horizontal arrow) and individual Macrophages (Mo), and, endothelial hypertrophy in a small epineural artery (E). **(F)** Axonal degeneration with digestion chambers
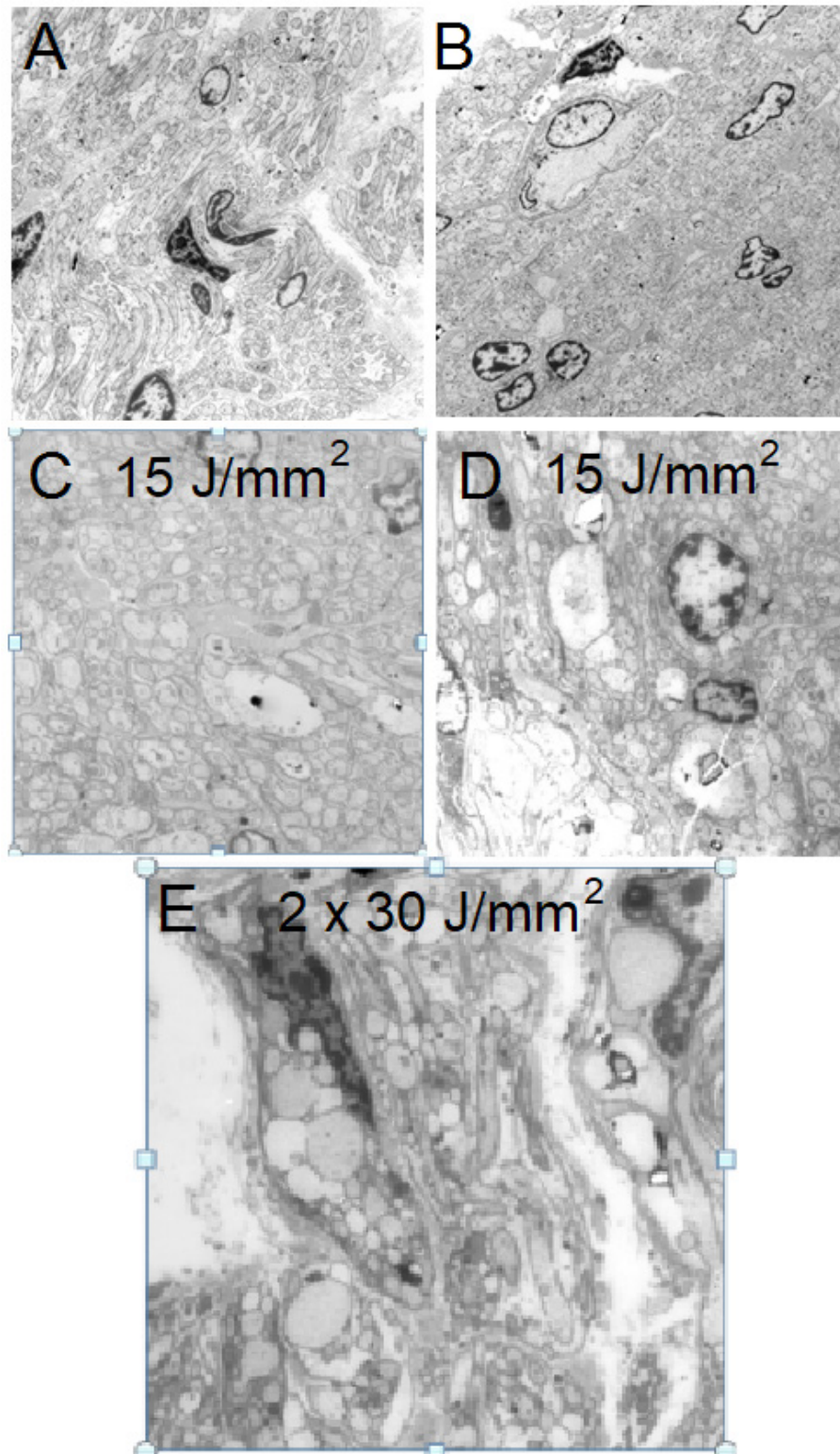
Figure 7: Sympathetic nerves examined electron microscopically **showing**: **(A)** and **(B)** Normal appearance of non-irradiated renal arteries, remak cluster with preserved physiological fibre density, with normal axoplasmatic organelles, cytoskeletal structure and Remak cells, as compared to: **(C)** and **(D)** 4 weeks after laser radiation *showing*: Remak cluster with anisometry of axons, axon segments with granular disintegration, and, **(E)** Severe distinctive axonal anisometry with various densities of the axonal cytoskeleton, and granular disintegration
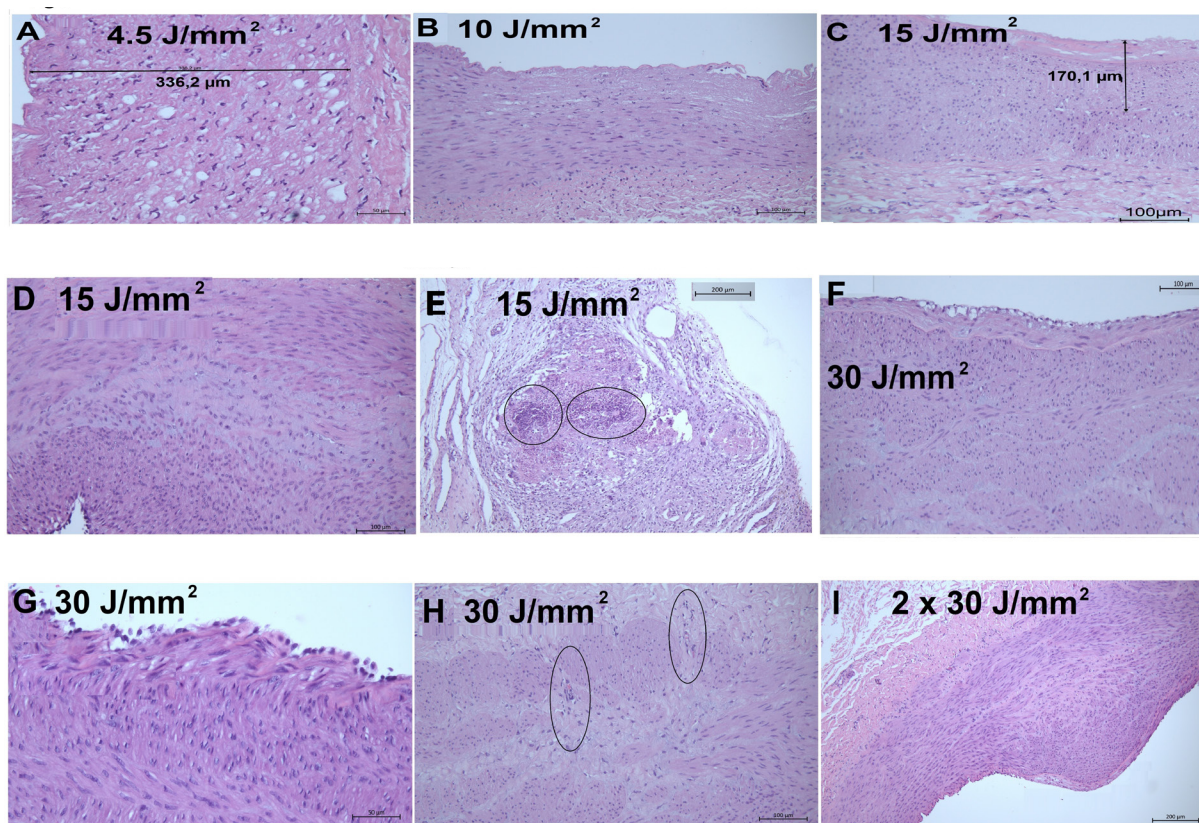
Figure 8: Acute laser induced lesions of renal arteries; Histopathology of the wall of renal arteries after intraluminal laser radiation *showing*: **(A)** Moderate thermal damages of the vessel media; **(B)** Mild focal thermal alteration of the intima and the upper layer of the media; **(C)** Minimal focal thermal alteration; **(D)** Focally reduced muscle fibres and collagen deposit in the vessel media; **(E)** Focal inflammatory infiltration and necrosis around denaturated tissue suggesting severely altered, coagulated sympathetic nerves; **(F)** Slight subendothelial vacuolization; **(G)** Arterial wall with altered fibre orientation in the superficial layers of the vessel media; **(H)** Scars of the fissured media (ovals) suggesting a healing process after mechanical injury by catheter manipulation; and **(I)** Focal eccentric hyperplasia of the intima and media, and small fibrotic scar in the media
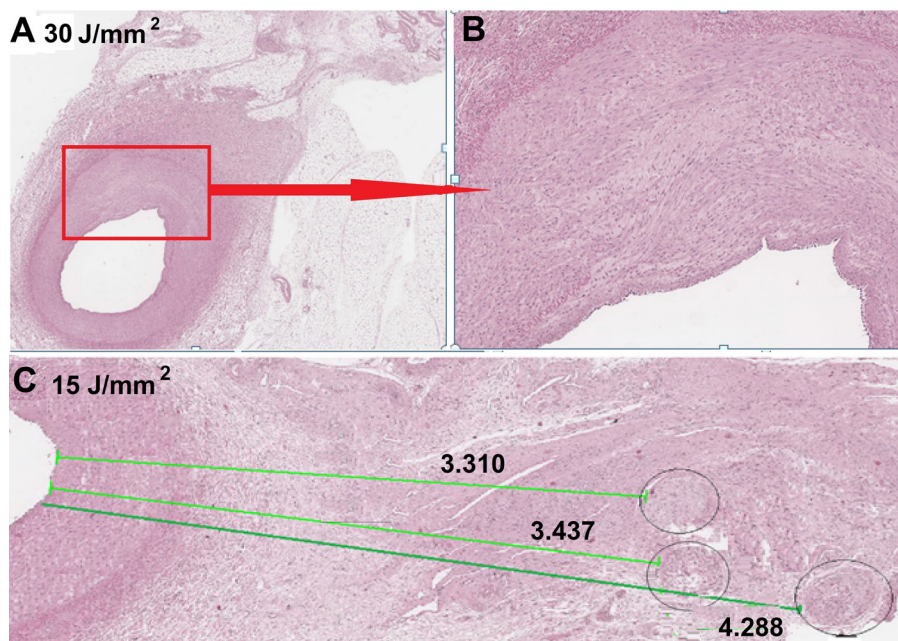

Figure 9: Cross section of the main left artery 31 days after catheter directed intraluminal laser radiation *showing*: **(A)** Preserved anatomical structure of the artery, without signs of fibrosis or narrowing of the lumen, without wall weakening with aneurysm formation; **(B)** Without thermal damage of the vessel layers; **(C)** Permanent thermal alteration of perirenal sympathetic nerves located at distances >4 mm from the inner lumen of the vessel

Discussion

As shown in this study, RSLD can achieve permanent renal sympathetic denervation selectively but only slight to moderate and reversible thermal damages to the renal artery and associated perivascular tissues. The 1064nm laser light has a low absorption in water so that the photons are intensely scattered, penetrating deep into perivascular tissue and inducing heat in tissue components selectively absorbing photons, whereas the catheter itself is not heated up. In contrast, transparent or translucent tissue such as the arterial wall is not or is only minimally absorbing photons and it is therefore less heated up, almost completely spared from thermally induced laser injuries. In addition, continuous catheter irrigation with saline at room temperature of 18 °C is washing around and cooling the inner lumen of the artery.

Catheter irrigation

Catheter irrigation is a prerequisite when using laser light in the cardiovascular system. It is needed for washing away the blood from the catheter endhole and creating a clear pathway for the laser beam aimed at the inner surface of the artery, and, to avoid blood penetration into the catheter endhole that may burn the fibre and destroy the catheter. Saline irrigation flow may explain the higher thermal effect in deeper tissue layers where cooling effect of intra-arterial saline flow is gradually reduced with the distance from the vessel wall [22-24]. Thus, preheated by previous laser impacts in the deeper tissue higher temperatures are achieved by additive heating effects of repeated laser applications.

The scattering dominant light propagation

The scattering dominant light propagation uses a probability distribution of the likelihood of the end-point of a photon after multiple scattering events, each changing the photon direction, ultimately terminated by photon absorption and eventually heat induction in the deeper layers of tissue [25,26]. The 1064nm Nd:YAG laser light is absorbed selectively by sensitive tissue components such as myoglobin, hemoglobin, as well as in cellular components such as ribosomes and organelles of the cells (nucleus, mitochondria, endoplasmatic reticulum, Golgi apparatus) thereby generating heat. Laser damages selectively nerves but may also cause selectively apoptosis in the nerves [27]. All these may explain the selective laser effects on the renal sympathetic nerves when using 1064 nm Nd:YAG laser light and when applying energy settings as described. These effects cannot be achieved by using other laser wavelength with a higher absorption coefficient in water [20], or by using other energy sources which in addition may cause severe adverse effects on tissue local to the side of treatment, on the artery as well as on soft tissue at distance [28-30].

In function of radiation times

In function of radiation times with the increase of tissue temperature incrementally thermal effects will occur, starting with reversible effects such as a slight edema and minimal tissue enzyme activation up to irreversible acute coagulation necrosis of tissues sensible for the 1064nm Nd:YAG laser light. As shown in this study, for a safe RSLD procedure the power should be limited to 15W and application times adapted to the irradiated surface of the artery inner lumen. In order to achieve deep thermal laser effects the choice of appropriate energy settings is crucial for the safety of RSLD procedure. By doing so, consecutive laser impacts at time intervals of 5-10s could increase depth of laser effects, causing permanent denervation, saving the artery from permanent damages. In addition also further increase of thermal effect is achieved by heat conduction.

We have not assessed

We have not assessed indicators of renal sympathetic function e.g. blood pressure, tyrosine hydroxylase expression, norepinephrine concentration [30]. We have assessed the effects of RSLD on perirenal nerves, the arterial wall and the periarterial tissues when applying various energy settings anatomically, histopathologically and electron-microscopically. We have focused on the determination of the depth of penetration of treatment related injury (necrosis) of nerves and of location, distance, and severity of periarterial tissue. To avoid the risk of bleeding during the 4 weeks of follow-up arterial lines for blood pressure measurement were not applied in then two animals scheduled for a 4 weeks follow-up, even during the acute experiment. In addition, hyperthermia and arrhythmia invalidated blood pressure measurements in other two pigs.

In healthy pigs nerves ≥50 μm in size aggregate within 2 mm from the distal artery lumen, while the largest nerves ≥500 μm are only seen in the proximal, but are located >4.5 mm from the lumen [31]. An anatomic study in human tissues showed that a substantial proportion of the sympathetic nerve fibres were located deeper in the peri-arterial soft tissue than in the lesion depth created by the conventional catheter-based renal sympathetic denervation systems [32]. Anatomical assessment of sympathetic periarterial renal nerves in man showed that the mean distance from artery lumen to nerve location is least in the distal segments but there were fewer nerves surrounding the distal segments compared with the proximal density of periarterial renal sympathetic nerve fibers. There is a clear predominance of efferent nerve fibers, with decreasing prevalence of afferent nerves from proximal to distal periarterial renal parenchyma [33].

Location of radiation

Based on the deeper penetration of the 1064nm Nd:YAG laser induced heat RSLD can be performed successfully by limiting laser applications to the main renal artery from its ramification down to its root without including its ramifications in the ablation procedure, in the same time avoiding transvascular laser damages to the kidney. Importantly, laser applications with the catheter in intimate contact with the ramifications of the renal artery the divergent and deeply penetrating laser beam will hit the perirenal nerves of the smaller renal arteries emerging from the ramification at a distance of several millimeters; thereby including their perirenal nerves in the denervation process.

As compared to other methods, for RSLD catheterization and denervation of each ramification branch of the renal artery for effective lesion placement is not needed [34]. This may save time and reduce risks and patients' burden. By using the catheter *RytmoLas®* one laser impact adapted to the vessel lumen can denervate the entire circumference of the renal artery at a length of 5 to 6 mm (Figure 10). Laser lesions are homogenous, smoothly contiguous, slightly overlapping. Thus, successful RSLD of an arterial segment up to 4 cm in length can be achieved with 5 to 6 laser applications at 15W/30-60s. A longer denervated vessel segment may also hinder reinervation as reported after other RSD methods [35].
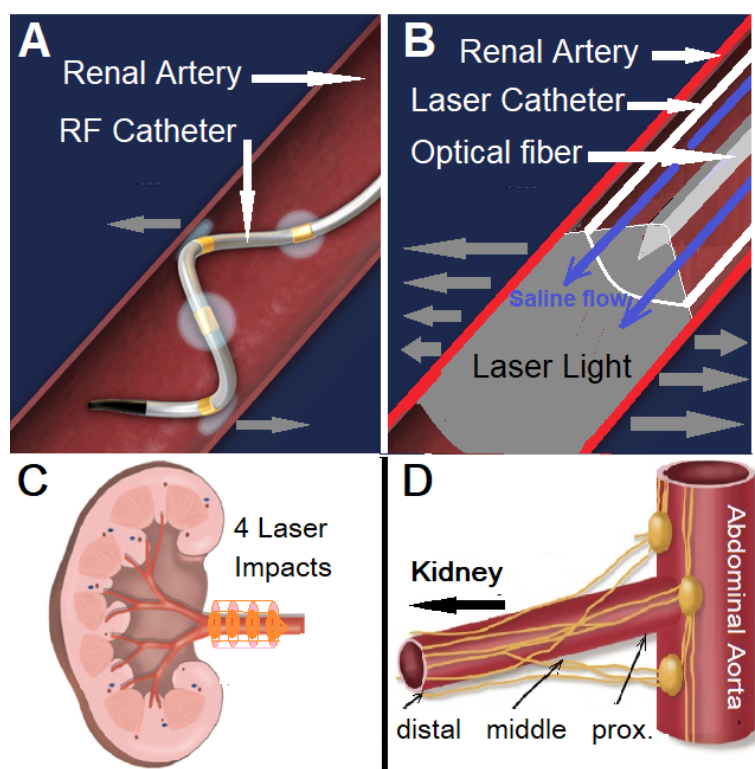

Figure 10: Scheme *showing:* **(A)** The method of renal denervation by using a spiral radiofrequency catheter. The hori-zontal grey arrows denote periarterial heat conduction from the point of radiofrequency current application; and **(B)** Segmental laser catheter radiation aimed at the inner lumen of the renal artery. Horizontal arrows show the heat generated by photon absorption and distribution into the periarterial tissue; **(C)** Locations of overlapping Laser impacts aimed at the inner lumen of renal arteries as applied in this study; **(D)** Renal artery and circumferential peri-arterial renal nerve location

Areas of investigation

RSLD affects both afferents and efferent sympathetic nerves decreasing renal noradrenaline release and in sympathetic nerve activity of the central nervous system and thereby to various organs including the cardiovascular system, diabetes, the kidneys, and pulmonary hypertension [36-39]. Recently, it has been reported that renal denervation added to catheter ablation in patients with paroxysmal atrial fibrillation and hypertension, compared with catheter ablation alone, significantly increased the likelihood of freedom from atrial fibrillation at 12 months [40]. This would open an intriguing new option for these patients because the *RytmoLas®* is designed and certified for intracardiac laser application and has already been successfully used for long-lasting atrial fibrillation ablation [41]. It would allow atrial fibrillation ablation and RSLD in one session by using the same catheter system, saving costs, procedural times, and interventional burden to the patient. In addition, besides the treatment of resistant hypertension and atrial fibrillation RSLD could emerge also as an effective therapy for other clinical conditions associated with chronically elevated sympathetic activity. In fact, a recent clinical study demonstrated that RD reduced monocyte activation, monocyte platelet aggregation, and circulating levels of several inflammatory cytokines and chemokines in hypertensive patients suggesting a direct connection between sympathetic activity and low-grade inflammation [42]. Currently, RSD is investigated in

diseases associated with increased sympathetic nerve activity, such as chronic kidney disease, heart failure with reduced ejection fraction, and arrhythmias, in particular in atrial fibrillation in combination with pulmonary vein isolation [43].

Conclusion

This represents yet another important area of investigation on the clinical benefits of RSLD. Provided clinical study trials can confirm these results RSLD may become an intriguing alternative for renal denervation by meeting best all of the requirements for catheter based renal denervation as outlined recently in the Proceedings from the 3rd European clinical consensus conference for clinical trials in device-based hypertensions therapies [44].

Conflict of interest

No potential conflict of interest declared

Acknowledgements

References

1. GBD 2013 Risk Factors Collaborators, Forouzanfar MH, Alexander L, Anderson HR, Bachman VF, et al. (2015) Global, regional, and national comparative risk assessment of 79 behavioral, environmental, occupational, and metabolic risk factors or clusters of risks in 188 countries, 1990–2013: a systematic analysis for the Global Burden of Disease Study 2013. Lancet 386: 2287-323.

2. Mills KT, Bundy JD, Kelly TN, Reed JE, Kearney PM, et al. (2016) Global disparities of hypertension prevalence and control: a systematic analysis of population-based studies from 90 countries. Circulation 134: 441-50.

3. Lawes CM, Vander Hoorn S, Rodgers A (2008) International Society of Hypertension. Global burden of blood-pressure-related disease. Lancet 371: 1513-8.

4. Danaei G, Finucane MM, Lin JK, Singh GM, Paciorek CJ, et al. (2011) Global Burden of Metabolic Risk Factors of Chronic Diseases Collaborating Group (Blood Pressure). National, regional, and global trends in systolic blood pressure since 1980: systematic analysis of health examination surveys and epidemiological studies with 786 coun-try-years and 5-4 million participants. Lancet 377: 568-77.

5. Addo J, Smeeth L, Leon DA (2007) Hypertension in sub-Saharan Africa: a systematic review. Hypertension 50: 1012-8.

6. Devi P, Rao M, Sigamani A, Faruqui A, Jose M, et al. (2013) Prevalence, risk factors and awareness of hyperten-sion in India: a systematic review. J Hum Hypertension 27: 281-7.

7. Egan BM, Zhao Y, Axon RN (2010) US trends in prevalence, awareness, treatment, and control of hypertension, 1988-2008. JAMA 303: 2043-50.

8. Kastarinen M, Antikainen R, Peltonen M, Laatikainen T, BarengoNC, et al. (2009) Prevalence, awareness and treat-ment of hypertension in Finland during 1982-2007. J Hypertension 27: 1552-9.

9. Cífková R, Skodová Z, Bruthans J, Holub J, Adámková V, et al. (2010) Longitudinal trends in cardiovascular mortality and blood pressure levels, prevalence, awareness, treatment, and control of hypertension in the Czech population from 1985 to 2007/2008. J Hypertension 28: 2196-203.

10. De la Sierra A, Segura J, Banegas JR, Gotostidi M, de la Cruz JJ, et al. (2011) Clinical features of 8295 patients with resistant hypertension classified on the basis of ambulatory blood pressure monitoring. Hypertension 57: 898-902.

11. Carey RM, Sakhuja S, Calhoun DA, Whelton PK, Muntner P (2019) Prevalence of Apparent Treatment-Resistant Hypertension in the United States. Comparison of the 2008 and 2018 American Heart Association Scientific Statements on Resistant Hypertension. Hypertension 73: 424-31.

12. Pimenta E, Calhoun DA (2012) Resistant hypertension: incidence, prevalence, and prognosis. Circulation 125: 1594-6.

13. Mancia G, Fagard R, Narkiewicz K, Redón J, Zanchetti A, et al. (2013) ESH/ESC guidelines for the management of arterial hy-pertension: the Task Force for the Management of Arterial Hypertension of the European Society of Hyper-tension (ESH) and of the European Society of Cardiology (ESC). J Hypertens 31: 1281-357.

14. Grassi G, Cattaneo BM, Seravalle G, Lanfranchi A, Mancia G (1998) Baroreflex control of sympathetic nerve activity in essential and secondary hypertension. Hypertension 3: 68-72.

15. Esler M, Lambert G, Jennings G (1989) Regional norepinephrine turnover in human hypertension. Clin Exp Hyper-tens A 11: 10.3109/10641968909045414.

16. Krum H, Schlaich M, Whitbourn R, Sobotka PA, Sadowski J, et al. (2009) Catheter-based renal sympathetic dener-vation for resistant hypertension: a multicentre safety and proof-of-principle cohort study. Lancet 373: 1223-310.

17. Townsend RR, Mahfoud F, Kandzari DE, Kario K, Pocock S, et al. (2017) Catheter-based renal denervation in pa-tients with uncontrolled hypertension in the absence of antihypertensive medications (SPYRAL HTN-OFF MED): a randomized, sham-controlled, proof-of-concept trial. The Lancet 390: 2160-70.

18. Kapil V, Jain AK, Lobo MD (2014) Renal Sympathetic Denervation - A Review of Applications in Current Practice. Interventional Cardiol Rev 9: 54-61.

19. Streitparth F, Walter A, Stolzenberg N, Heckmann L, Breinl J (2013) MR-guided perirenal ethanol injection for re-nalsympathetic denervation: A feasibility study in pigs. Cardiovasc Interventional Radiol 36: 791-6.

20. Alexander VV, Shi Z, Iftekher F, Welsh MJ, Gurm HS (2014) Renal Denervation Using Focused Infrared Fiber Lasers: A Potential Treatment for Hypertension. Lasers Surg Med 46: 689-702.

21. Weber H, Schmitz L, Heinze A, Ruprecht L, Sagerer-Gerhardt M (2017) The development of a laser catheter with improved mapping resolution and online monitoring of lesion formation during arrhythmia ablation In: Bellucci C (edi-tor) Laser Ablation. Advances in Research and Applications. Nova Science Publishers, New York, USA.

22. Weber H, Sagerer-Gerhardt M (2013) Open-irrigated laser catheter ablation produces flow-dependent sizes of le-sions. Pacing Clin Electrophysiol 36: 1132-7.

23. Weber H, Sagerer-Gerhardt M (2014) Open-irrigated laser catheter ablation: relationship between the level of ener-gy, myocardial thickness, and collateral damages in a dog model. Europace 16: 142-8.

24. Weber H, Sagerer-Gerhardt M (2014) Open-irrigated laser catheter ablation: Influence of catheter irrigation and of contact and non-contact mode of laser application on lesion formation in Bovine myocardium. Lasers Med Sci 29: 1183-7.

25. Splinter R (2015) Laser catheter ablation of cardiac arrhythmias: Experimental and basic research and clinical re-sults. In: Topaz On (editor), Lasers in Cardiovascular Interventions, Springer London Ltd, UK.

26. Weber H, Sagerer-G M (2015) Laser-based approach to cardiac mapping and arrhythmia ablation, In: Topaz On (editor), Lasers in Cardiovascular Interventions, Springer London, UK.

27. Schlegel F, Daneschnejad SS, Mavlikeev M, Klein S, Vollroth M, et al. (2014) Early effects in perivascular nerves and atrial media following renal artery denervation. Hypertension 63: 123-5.

28. Aguila FJM, García JDM, Navarro EM, Hitos JAV, Fernández-Torres C (2014) Bilateral renal artery stenosis after renal denervation. Hypertension 63: e126-e127.

29. Sakaoka A, Terano H, Nakamura SH, Hagiwara H, Furukawa T, et al. (2018) Accurate depth of radiofrequency-induced lesions in renal sympathetic denervation based on a fine histological sectioning approach in a porcine model. Circ Cardiovasc Interv 11: 1-8.

30. Sakakura K, Ladich E, Edelmann ER, Markham P, Stanley JRL, et al. (2014) Methodological standardization for the pre-clinical evaluation of renal sympathetic denervation. JACC 7: 1184-93.

31. Yahagi K, Ganey C, Mori H, Koppara T, Lutter CH, et al. (2016) Anatomical considerations for renal denervation: Peri-arterial nerve size distribution in healthy swine (Abstract). JACC 67.

32. Choe W-S, Song WH, Jeong CW, Choi E-K, Oh S (2019) Anatomic Conformation of Renal Sympathetic Nerve Fibers in Living Human Tissues. Sci Rep 9: 10.1038/s41598-019-41159-4.

33. Sakakura K, Ladich E, Chen Q, Otsuka F, Yahagi K, et al. (2014) Anatomic assessment of sympathetic peri-renal nerves in man. J Am Coll Cardiol 64: 635-43.

34. Felix Mahfoud F, Tunev ST, Ewen S, Cremers B, Ruwart J, et al. (2015) Impact of Lesion Placement on Efficacy and Safety of Catheter-Based Radiofrequency Renal Denervation. JACC 66: 1766-75.

35. Booth LC, Nishi EE, Yao ST, Ramchandra R, Lambert GW, et al. (2015) Reinervation of renal afferent and efferent nerves at 5.5 and 11 months after catheter-based radiofrequency renal denervation in sheep. Hypertension 65: 393-400.

36. Ester M (2014) Illusions of truths in the Simplicity HTN-3 trial: generic design strengths but neuroscience failings. J Am Soc Hypertens 8: 593-8.

37. Grassi G, Seravalle G, Brambilla G, Trabattoni D, Cuspidi C, et al. (2015) Blood pressure responses to renal dener-vation precede and are independent of the sympathetic and baroreflex effects. Hypertension 65: 1209-16.

38. Schlaich M, Hering D, Lambert G, Lambert E, Eslaer M (2015) Blood pressure and sympathetic nervous system re-sponse to renal denervation. Hypertension 65: 393-400.

39. Rothman AMK, Arnold ND, Chang W, Watson O, Swift AJ, et al. (2015) Pulmonary artery de-nervation reduces pulmonary artery pressure and induces histological changes in an acute porcine model of pulmo-nary Hypertension. Circ Cardiovasc Interv 8: 1-7.

40. Steinberg JS, Shabanov V, Ponomarev D, Losik D, Ivanicki E, et al. (2020) Effect of Renal denervation and catheter ablation vs catheter ablation alone on atrial fibrillation recurrence among patients with paroxysmal atrial fibrillation and hypertension: The ERADICATE-AF randomized clinical trial. JAMA 323: 248-55.

41. Weber H, Sagerer-Gerhardt M, Heinze A (2017) Laser catheter ablation of long-lasting persistent atrial fibrillation: Longterm results. JAFIB 10: 1-10.

42. Zaldivia MT, Rivera J, Hering D, Marusic P, Sata Y, et al. (2017) Renal denervation reduces monocyte activation and monocyte-platelet aggregate formation: an anti-inflammatory effect relevant for cardiovascular risk. Hypertension 69: 323-31.

43. Lauder L, Boehm M, Mahfoud F (2020) Where is renal nerve ablation going? European Heart Journal 41: 4538-40.

44. Mahfoud F, Azizi M, Ewan S, Pathak A, Ukena CH, et al. (2020) Proceedings from the 3rd European clinical con-sensus conference for clinical trials in device-based hypertensions therapies. Eur Heart J 41: 1588-99.